

Identification of a ubiquitination-based classification system and a gene signature for predicting prognosis and immunotherapy response for sarcoma

Lin Zhang

Renmin Hospital of Wuhan University

Weihao Lin

National Cancer Center, Chinese Academy of Medical Sciences and Peking Union Medical College

Zheng Cao

National Cancer Center, Chinese Academy of Medical Sciences and Peking Union Medical College

Xiaoli Feng

National Cancer Center, Chinese Academy of Medical Sciences and Peking Union Medical College

Yibo Gao (✉ gaoyibo@cicams.ac.cn)

National Cancer Center, Chinese Academy of Medical Sciences and Peking Union Medical College

Jie He

Renmin Hospital of Wuhan University

Research Article

Keywords: Sarcomas, Ubiquitination, TRIM21, TCGA, Immunotherapy, Tumor microenvironment, Gene signature, Prognosis

Posted Date: May 13th, 2022

DOI: <https://doi.org/10.21203/rs.3.rs-1641963/v1>

License:   This work is licensed under a Creative Commons Attribution 4.0 International License.

[Read Full License](#)

Abstract

Background: Sarcomas are heterogeneous tumors deriving from the mesenchyme and have a poor response to systemic therapies. Ubiquitination is a post-translational modification that is involved in various physiological processes and cancer growth.

Methods: We integrated the transcriptome data of 256 sarcoma patients from The Cancer Genome Atlas (TCGA) to analyze the expression of the predefined ubiquitin-related genes and identified two ubiquitin-related clusters based on that. Patients' survival, enrichment analysis, and tumor microenvironment analyses were conducted. Further, a ubiquitin-related gene signature was built to predict prognoses. The prognostic value of the signature was also validated in public datasets. Pathway analysis, and tumor microenvironment characterization were conducted between different risk groups. The prognostic values of the signature were partly verified using immunohistochemistry assay in an independent cohort from our center.

Results: The two clusters were characterized by different survival outcomes, enriched pathways, and characteristics of the tumor microenvironment. The signature could effectively predict patient prognoses across TCGA sarcoma cohort, and another two public sarcoma cohorts. Different risk groups were also characterized by distinct enriched pathways and characteristics of the tumor microenvironment. Histochemistry score analyses revealed that patients with a higher TRIM21 expression had a significantly better prognosis, and higher TRIM21 combined with higher CD8 was also significantly associated with better overall survival.

Conclusions: This study provided novel classification for sarcoma patients based on expressions of ubiquitin-related genes. The classification and the constructed gene signature may facilitate the understanding of sarcoma pathogenesis, prediction of prognosis and immunotherapy response for sarcoma patients.

Introduction

Sarcoma is a heterogeneous group of rare malignant tumors that originate from mesenchymal tissues and can be divided into soft-tissue and bone sarcomas.(1) Although accounting for only a small proportion (<1%) of all malignant tumors, it consists of more than 100 subtypes.(1-3) To date, surgical management with or without adjuvant/neoadjuvant radiotherapy remains the first-line treatment for localized soft tissue sarcomas, and chemotherapy is an additional option for high-risk patients.(2, 3) Sarcomas have a poor prognosis and a high mortality, which may be due to the insensitivity to traditional chemotherapy, invasive nature and easy recurrence of some subtypes.(2, 3) Therefore, identification of sarcoma patients with different prognoses and treatment sensitivities will improve the understanding of these diverse tumors and facilitate individualized therapies.

Post-translational modifications (PTMs) are regulatory events that modulate the activity of proteins enzymatically.(4) Ubiquitination is a reversible PTM that is involved in regulating protein function or

degradation by the proteasome and participates in multiple cellular and biological processes.(5) Ubiquitination could be achieved by conjugating to the lysine residues of substrate proteins by an enzymatic cascade, including E1 activation enzymes, E2 conjugation enzymes, and E3 ubiquitin ligases. (6) The ubiquitination process could also be reversed by deubiquitinating enzymes that removes ubiquitin from substrates.(7) Studies have shown that dysregulation of the ubiquitination system plays a key role in many diseases, including neurodegenerative diseases, autoimmune diseases, and cancers.(7)

Interactions between the ubiquitin system and sarcomas have been reported in previous studies. For example, TRIM21 could positively regulate osteosarcoma cell proliferation and differentiation,(8, 9) TRIM8 is a selective dependency gene in Ewing sarcoma and regulates EWS/FLI protein expression as an E3 ligase, controlling the growth and apoptosis of Ewing sarcoma.(10) However, the roles of ubiquitin-related genes (URGs) in sarcomas have not been fully investigated. A better understanding of the underlying mechanisms may facilitate future research of sarcomas. In this study, we integrated transcriptional and clinical data of The Cancer Genome Atlas (TCGA) sarcoma cohort (TCGA-SARC) to systematically explore the prognostic values of ubiquitin-related genes in TCGA-SARC patients. We identified two distinct ubiquitin-related clusters that were characterized by distinct patient prognoses, enriched pathways and tumor environment; further, we built a ubiquitin-related gene signature that could effectively predict the prognosis and immunotherapy of sarcoma patients. In addition, the conclusions were partly validated in a sarcoma cohort from our center. Hopefully, the characterization of different clusters and establishment of the signature could help to better understand sarcoma pathogenesis and facilitate prognostic management and risk stratification for sarcoma patients.

Materials And Methods

Data source

The gene expression matrices of sarcomas with paired clinical data are downloaded in The Cancer Genome Atlas database (<https://portal.gdc.cancer.gov/>). After excluding normal samples, relapsed or metastatic tumors, 256 cases were included in the final analyses. The clinical data and gene expression files of 85 osteosarcoma patients derived from the osteosarcoma cohort from the TARGET database (TARGET-OS, (<https://ocg.cancer.gov/programs/target/projects/osteosarcoma>)) were used as a validation cohort. GSE17674 microarray data on 44 Ewing sarcoma cases were downloaded from the GEO database (<https://www.ncbi.nlm.nih.gov/geo/>) and these patients were used as another validation cohort. The data were normalized and $\log_2(X+1)$ transformed.

List of ubiquitin-related genes

A list of 807 URGs was collected from the iUUCD 2.0 database (<http://iuucd.biocuckoo.org/>).(11, 12) After matching with the mRNA expression profiles from TCGA-SARC dataset, 802 URGs were extracted. The genes were then screened with the standard of >1 transcripts per kilobase, and the remaining 752 genes were incorporated into final analyses (**Table S1**).

Screening for sarcoma subtypes and enrichment analysis

On the basis of the expression profiles of ubiquitin-related genes, molecular subtypes were clustered and identified using the nonnegative matrix factorization (NMF) R package.(13) The clustering was performed using the following settings: “brunet” option, and 100 iterations. The optimal cluster number was determined according to the cophenetic, dispersion, and silhouette coefficients. Gene set variation analyses (GSVA) were performed with the GSVA R package to investigate the pathways correlated with the different sarcoma subtypes. The gene sets of “h.all.v7.2.symbols” was downloaded from MSigDB and used for enrichment analysis.(14)

Tumor microenvironment analysis

The epithelial-mesenchymal transition (EMT) score was calculated based on the EMT gene signature, as previously described.(15) Key immune characteristics,(16) including leukocyte fraction, stromal fraction, SNV neoantigen, Indel neoantigen, T-cell receptor (TCR) Shannon and TCR richness were downloaded from the website (<https://gdc.cancer.gov/about-data/publications/panimmune>) and were compared between distinct ubiquitin-related clusters or between high and low risk groups. Immune infiltration analyses were performed using TIMER 2.0 (<http://timer.comp-genomics.org/>), with the CIBERSORT algorithm, absolute mode.(17, 18)

Establishment and evaluation of a ubiquitin-related signature

Univariate Cox analysis and random survival forest analysis were performed sequentially to establish a ubiquitin-related prognostic signature, as previously described.(15) The risk score was calculated as follows: risk score = $\sum(C_i \times \text{Exp}_i)$; ‘C’ stands for the coefficient of genes and ‘Exp’ is their expression levels. All the patients in different cohorts were divided into high and low risk groups, based on their median risk scores. Time-dependent receiver operator characteristic (ROC) curves were drawn to evaluate the prognostic prediction efficacy of the signature.

Sample collection

The study was performed with the approval of the Ethics Committee of Cancer Hospital, Chinese Academy of Medical Sciences. Specimens of sarcomas were obtained from 50 patients in Cancer Hospital, Chinese Academy of Medical Sciences. Waiver of informed consent was obtained from the same committee in consideration of the retrospective nature of the study.

Immunohistochemistry and quantification

Immunohistochemistry was performed as previously described.(19) The primary antibodies used were rabbit anti-TRIM21 (dilution 1:200; Proteintech, 12108-1-AP) and mouse anti-CD8 (dilution 1:4000; Proteintech, 66868-1-Ig). The secondary antibodies were peroxidase labeled anti-rabbit IgG (H+L) antibody (dilution 1:200; SeraCare, 5220-0336) and peroxidase labeled anti-mouse IgG (H+L) antibody (dilution 1:200; SeraCare, 5220-0341). The expressions of proteins were quantitated using an H-score, as

was applied previously.(19, 20) The H-score was recorded as the product of 2 parameters: percent of positive cells (0: 0-10%, 1: 11%-40%, 2: 41-70%, 3: 71%-100%) and intensity of staining (0=very weak, 1 = weak, 2 = moderate, 3 = strong). The results were validated by two pathologists (Z.C. and X.F.) who were blinded to the clinical information of patients.

Statistical analysis

R software v.3.6.1, GraphPad Prism 8.0, and Stata 16.0 were used to analyze data and plot figures. Wilcoxon test and Kruskal–Wallis test were applied for comparisons of two and three groups, respectively. Univariate Cox regression analyses were performed by the corresponding R packages. The Kaplan–Meier method and Log-rank tests were used to evaluate the difference of survival outcomes between different clusters or risk groups with the R package “survminer” and “survival”. A p value < 0.05 (two-tailed) was considered statistically significant.

Results

Identification and characterization of two ubiquitin-related subgroups

The detailed workflow was shown in **Figure S1**. Among 752 URGs, 138 prognostic-related URGs were identified by univariate Cox analyses (**Figure 1A, Table S2**). NMF clustering was performed to classify sarcoma patients based on the expression of 138 URGs using TCGA-SARC. $K = 2$ was selected as the best cutoff based on the NMF algorithm, which means that patients from TCGA-SARC were classified into two clusters (**Figure S2**). A survival analysis revealed that the overall survival (OS) of patients in cluster 2 was better than that in cluster 1 ($p < 0.0001$; **Figures 1B**).

We further investigated the correlation between the two clusters and clinicopathological features in the TCGA cohort. The relevance between clinical characteristic and expression levels of the URGs in clusters 1 and 2 are shown in the heat map (**Figure 1C**). The enriched pathways were also analyzed by GSVA (**Table S3**) and the results were shown in a heat map in **Figure 1D**. We noticed that the EMT pathway was enriched in cluster 1. Therefore, we calculated the EMT score of the two clusters, and observed a higher EMT score in cluster 1 (**Figure 1E**). The results have implicated an activated immune response for cluster 2, which might account for its better survival and was explored in subsequent analyses.

Characterization of the tumor microenvironment of the two clusters

To understand the characteristics of the immune infiltration, we performed CIBERSORT. The distribution of immune cells (listed in **Table S4**) and its relationship with some clinical parameters of the two clusters were shown in a heat map in **Figure 2A**. Specifically, cluster 2 was characterized by higher infiltration levels of CD8+ T cells, and a higher M1/M2 macrophage proportion (**Figure 2B,C**).

We then evaluated the expressions of key immune characteristics (including leukocyte fraction, stromal fraction, single nucleotide variant neoantigens, indel neoantigens, TCR Shannon and TCR richness) and major histocompatibility complex (MHC) class II genes. Leukocyte fraction, stromal fraction, TCR

Shannon and TCR richness were significantly higher in cluster 2 (**Figure 2D**). Meanwhile, most of the MHC class II genes were also higher in cluster 2 (**Figure 2E**).

We also evaluated the expression of several prominent checkpoints, including CD274, TIGIT, PDCD1, CTLA4, LAG3, BTLA, and HAVCR2. The expressions of these checkpoints were all significantly higher in cluster 2 (**Figure 2F**), indicating the possibility of a better response to immunotherapy for this cluster.

Establishment and evaluation of a ubiquitin-related signature

From 752 URGs, 59 candidate genes with significant prognostic values ($p < 0.01$) were identified by univariate analyses (**Figure S3A**). Random survival forest analyses were then implemented to narrow the scope of candidate genes and the top 10 genes ranked by importance were selected for combination analysis and model construction (**Figure S3B**). The top 10 combinations with the smallest p values were shown in **Figure S3C**. Among them, the combination with the least gene number (LRRC41, RNF125, TRIM21 and UBE3D) was selected for building the final signature. The risk score was calculated using the following formula: risk score = $0.587057893868294 \times \text{LRRC41} + (-0.227071632803124) \times \text{RNF125} + (-0.54040867418788) \times \text{TRIM21} + 0.418750359339415 \times \text{UBE3D}$. The prognostic values of the four genes were investigated and all of them showed a significant prognostic value in patients from TCGA-SARC (**Figure S3D**).

Further, the prognostic values of the signature was explored in three public datasets. First, the patients in TCGA-SARC (training cohort) were assigned to a high risk or a low risk group according to the median risk score (**Figure 3A**). The survival analysis revealed that patients in the low risk group had significantly better OS (**Figure 3D**). The areas under the ROC curve for OS were 0.745 at 2 years, 0.762 at 3 years, and 0.743 at 5 years (**Figure 3G**). The risk scores were then calculated likewise for patients from two validation cohorts (**Figure 3B** for TARGET-OS and **Figure 3C** for GSE17674), and patients in low risk groups all had significantly better prognoses (**Figure 3E,F**). Analyses of the 2-year, 3-year, and 5-year prognostic prediction abilities indicated that the model had relatively strong robustness and effectiveness (**Figure 3H,I**).

Pathway analyses and tumor microenvironment characterization in different risk groups

We explored the correlations between the clustering system and the signature. Changes in the attributions of individual sarcoma patients from TCGA-SARC in different clusters, risk subgroups, and survival status were shown in an alluvial diagram; the diagram showed that cluster 1 patients had the highest proportion of the high risk subtype and was linked to a higher incidence of fatality (**Figure 4A**). Correspondingly, the mean risk score of patients in cluster 1 was significantly higher than cluster 2 (**Figure 4B**). We then further investigated the enriched pathways related to the signature. GSEA showed that pathways including glycolysis, unfolded protein response, MYC targets V2, MYC targets V1, G2M checkpoint, E2F targets were enriched in the high risk group (**Figure 4C**). Interestingly, we noticed that hallmark of EMT was also enriched in the high risk group (**Figure 4D**). Therefore, differential expressions of EMT-related genes were explored in the two groups. Among 8 EMT-related genes, 7 were significantly higher in the high risk group,

while 1 (CDH1) was lower in that group (**Figure 4E**). Consistently, EMT score was significantly higher in the high risk group (**Figure 4F**). We also performed GSVA, which revealed the correlation between risk score and the known biological processes (**Table S5**). Interestingly, risk score was negatively correlated with CD8 T effector pathway, antigen processing machinery, and immune checkpoint (**Figure 4G**). Based on this, relative pathways were further explored.

To further understand the underlying mechanisms, the tumor microenvironment of the two risk groups was characterized. Firstly, Spearman's correlation analyses were performed to explore the correlations between risk score, each signature gene and immune cell infiltration; a widespread correlation between the expression of the genes, risk score, and immune cell infiltration was observed (**Figure 5A**). Specifically, CD8+T cells and M1/M2 macrophage proportion were significantly higher in the low risk group (**Figure 5B,C**), which is in line with the GSVA result. Consistent with this, GSEA revealed an enrichment of hallmark of interferon gamma response in the low risk group and an enrichment of hallmark of TGF beta signaling in the high risk group (**Figure 5D,E**). According to the GSVA result, we further tested the major MHC class II genes, and most of them showed a higher expression in the low risk group (**Figure 5F**). Additionally, the expressions of several prominent checkpoint genes in different risk groups were examined, and significantly higher levels of CTLA4, PDCD1, BTLA, TIGIT, HAVCR2, CD274, LAG3 were observed in the low risk group (**Figure 5G**). The results implicated that patients in the low risk group may have a better response to immunotherapy.

Analyses for TRIM21 and validation in our cohort

One of the signature gene, TRIM21, is an E3 ubiquitin ligase that is well known to be involved in innate immunity and cancer proliferation.⁽²¹⁾ Therefore, we further analyzed the potential role of it in sarcomas. Enrichment analysis showed that hallmark of interferon-gamma response was enriched in patients with high TRIM21 (**Figure 6A**). Correlation analysis showed that TRIM21 was positively correlated with several prominent checkpoint genes such as CD274, LAG3, TIGIT, BTLA, CTLA4, PDCD1, and HAVCR2 (**Figure 6B,C**). Intriguingly, TRIM21 was also correlated with CD8+ T cells (**Figure 6D**). To partly validate the above conclusions, we retrospectively collected the specimens of 50 sarcoma patients from Cancer Hospital, Chinese Academy of Medical Sciences and performed immunohistochemistry assays to analyze the expressions of related proteins. The clinical information of these patients has been listed in **Table S6**. We analyzed the expressions of TRIM21 and CD8. Significantly, the expression of TRIM21 was positively correlated with that of CD8 (**Figure 6F**). We have also analyzed the prognostic values of them, and observed that a higher expression of TRIM21 was significantly related to better patients' survival. (**Figure 6G**). Although the association between a higher expression of CD8 protein and better patients' survival was not significant, higher TRIM21 combined with higher CD8 was significantly associated with better OS (**Figure 6H,I**). Representative images of IHC were shown in **Figure 6E**.

Discussion

Sarcomas are a group of invasive and heterogeneous mesenchymal tumors that have a poor response to current systemic therapies. The current situation of sarcomas has highlighted the urgent need for models for risk stratification and immunotherapy efficacy prediction. In this study, ubiquitin-related genes were integrated to identify different molecular clusters in sarcoma patients and a gene signature was built to stratify the risk levels of patients with sarcomas.

Based on the prognostic values of the 138 URGs, patients from TCGA-SARC were classified into two clusters. The survival outcomes, enriched pathways, TME characteristics were distinct between them. Patients in cluster 2 have better survival, and the enriched pathways identified by GSVA include interferon alpha response, interferon beta response, complement, indicating an activated immune response. So we further explored the tumor microenvironment, revealing higher levels of CD8 + T cells and a higher M1/M2 macrophage proportion, higher leukocyte fraction and stromal fraction in cluster 2; also, higher levels of MHC class II genes and immune checkpoints were observed in this cluster. The results were consistent with previous research which revealed that the group with higher levels of CD8 + and macrophages was related to better survival.(22) They were also in line with a previous study, showing that the group with better survival had higher levels of MHC class II genes.(23) The integrated effects of higher immune infiltration, high expression levels of immune parameters, and a lower EMT score, may be responsible for the worse survival in cluster 1. The effects, together with higher levels of checkpoints, indicated an immune-inflamed tumor microenvironment for cluster 2, and implicated a higher susceptibility to immunotherapy.

To accurately evaluate the risk of individual patients on the ubiquitination basis, a prognostic signature was developed using four ubiquitin-related genes that were all significantly correlated with the survival of patients in TCGA-SARC. The signature could effectively distinguish high and low risk patients from TCGA-SARC, TARGET-OS and GSE17674. Likewise, the enriched pathways, immune infiltration and EMT scores were distinct between the two risk groups. Patients in the high risk group were correlated with lower expressions of most MHC class II genes, lower levels of CD8 + T cells, a lower M1/M2 macrophage proportion, and lower levels of checkpoints. These patients are also enriched in hallmark of EMT and TGF beta signaling. Therefore, the above results may have implicated that the ubiquitination-related genes play a critical role regulating the development of sarcoma and mediating the clinical response to immunotherapy of these patients.

Among the four genes, RNF125 and TRIM21 were protective, while LRR41 and UBE3D were risk factors. Among them, TRIM21 positively regulates the proliferation of osteosarcoma and is involved in the senescence of it.(8, 24) TRIM21 is also involved in osteosarcoma cell autophagy and subsequent differentiation.(9) For the other three genes, no relevant studies were reported in sarcomas. However, some have been reported in other tumors. For example, RNF125 was down-regulated in BRAF inhibitor-resistant melanomas and participates in the chemoresistance of melanoma to BRAF inhibitors;(25) LRR4 could act as an autophagy inhibitor and restores the sensitivity of glioblastomas to temozolomide; LRR4 could also inhibit the proliferation of glioblastoma cells via circular RNAs.(26, 27)

UBE3D has not been reported in tumors yet. These genes may represent novel therapeutic strategies for sarcoma treatment and further studies are needed to examine the function of them in sarcomas.

The EMT is defined as the reprogramming of cells from an epithelial phenotype into a mesenchymal phenotype and is characterized by the loss of intercellular interaction and a lack of polarity, as well as increases in extracellular matrix interfaces, for the convenience of invasion and migration.(28) In this study, we observed that the hallmark of EMT was an enriched pathway in cluster 1 and the high risk group. Consistently, a higher EMT score was identified in them. Since sarcomas are malignant tumors arising from mesenchyme, they are already equipped with the mesenchymal phenotypic features and do not need to undergo the EMT process.(29) A possible explanation is that the metastable phenotype between the epithelial and mesenchymal stages enables sarcomas to undergo the EMT process under specific conditions, and contributes to their aggressive clinical behaviors.(29) These behaviors then lead to a worse clinical outcome.

There are some limitations. First, this is a retrospective study, based mainly on publicly available datasets. Second, the prognostic values of the signature have just been partly verified due to the rarity of samples, there is no condition for continued or further verification; the prediction for response to immunotherapy was not validated, either, because of the lack of immunotherapy cohorts. A prospective study with a large sample size of patients with sarcomas is needed for further external validation. Third, functional studies are still in need to elucidate the precise roles of ubiquitin-related genes in the development of sarcomas.

Conclusions

In conclusion, our study established a new classification system for sarcomas based on the expression profiles of ubiquitin-related genes, and a prognostic gene signature was built, providing a tool for risk stratification and prognosis management in sarcoma patients. The study has also partly revealed the correlation between the URGs and the tumor microenvironment in sarcomas, providing clues for future research.

Abbreviations

EMT: epithelial-mesenchymal transition;

GSVA: gene set variation analyses;

MHC: major histocompatibility complex;

NMF: nonnegative matrix factorization;

OS: overall survival;

PTMs: post-translational modifications;

ROC: receiver operator characteristic;

TARGET-OS: the osteosarcoma cohort from the TARGET database;

TCGA: The Cancer Genome Atlas;

TCGA-SARC: TCGA sarcoma cohort;

TCR: T-cell receptor;

URGs: ubiquitin-related genes

Declarations

Funding

This work was supported by the National Key R&D Program of China (2021YFF1201300), National Natural Science Foundation of China (82122053, 82188102), CAMS Initiative for Innovative Medicine (2021-I2M-1-067), Non-profit Central Research Institute Fund of Chinese Academy of Medical Sciences (2021-PT310-001, 2021-RC310-020), Key-Area Research and Development Program of Guangdong Province (2021B0101420005).

Author's contributions

All authors have made significant contributions to this work and approved the final version of this paper.

Acknowledgements

None.

Data availability statement

The datasets used in the current study are available from the corresponding author on reasonable request.

Declarations

Conflict of interest

The authors declare that they have no conflict of interest.

Ethics approval

The study was performed with the approval of the Ethics Committee of Cancer Hospital, Chinese Academy of Medical Sciences. Waiver of informed consent was obtained from the same committee in consideration of the retrospective nature of the study.

Informed consent

Not applicable.

References

1. Zhu MMT, Shenasa E, Nielsen TO. Sarcomas: Immune biomarker expression and checkpoint inhibitor trials. *Cancer Treat Rev* 2020;91:102115. [http://doi.org/ 10.1016/j.ctrv.2020.102115](http://doi.org/10.1016/j.ctrv.2020.102115).
2. Meyer M, Seetharam M. First-Line Therapy for Metastatic Soft Tissue Sarcoma. *Curr Treat Option On* 2019;20(1)[http://doi.org/ 10.1007/s11864-019-0606-9](http://doi.org/10.1007/s11864-019-0606-9).
3. Yuan J, Li X, Yu S. Molecular targeted therapy for advanced or metastatic soft tissue sarcoma. *Cancer Control* 2021;28:544350640. [http://doi.org/ 10.1177/10732748211038424](http://doi.org/10.1177/10732748211038424).
4. Chiang C, Gack MU. Post-translational Control of Intracellular Pathogen Sensing Pathways. *Trends Immunol* 2017;38(1):39-52. [http://doi.org/ 10.1016/j.it.2016.10.008](http://doi.org/10.1016/j.it.2016.10.008).
5. Nakamura N. Ubiquitin System. *Int J Mol Sci* 2018;19(4):1080. [http://doi.org/ 10.3390/ijms19041080](http://doi.org/10.3390/ijms19041080).
6. Deng T, Hu B, Wang X, et al. TRAF6 autophagic degradation by avibirnavirus VP3 inhibits antiviral innate immunity via blocking NFKB/NF-κB activation. *Autophagy* 2022;ahead-of-print(ahead-of-print):1-18. [http://doi.org/ 10.1080/15548627.2022.2047384](http://doi.org/10.1080/15548627.2022.2047384).
7. Yang G, Zhang X, Su Y, et al. The role of the deubiquitinating enzyme DUB3/USP17 in cancer: a narrative review. *Cancer Cell Int* 2021;21(1)[http://doi.org/ 10.1186/s12935-021-02160-y](http://doi.org/10.1186/s12935-021-02160-y).
8. Zeng QZ, Liu WT, Lu JL, et al. YWHAZ Binds to TRIM21 but Is Not Involved in TRIM21-stimulated Osteosarcoma Cell Proliferation. *Biomed Environ Sci* 2018;31(3):186-96. [http://doi.org/ 10.3967/bes2018.024](http://doi.org/10.3967/bes2018.024).
9. Zhang H, Zeng Q, Wu B, et al. TRIM21-regulated Annexin A2 plasma membrane trafficking facilitates osteosarcoma cell differentiation through the TFEB-mediated autophagy. *Cell Death Dis* 2021;12(1)[http://doi.org/ 10.1038/s41419-020-03364-2](http://doi.org/10.1038/s41419-020-03364-2).
10. Seong BKA, Dharia NV, Lin S, et al. TRIM8 modulates the EWS/FLI oncoprotein to promote survival in Ewing sarcoma. *Cancer Cell* 2021;39(9):1262-78. [http://doi.org/ 10.1016/j.ccell.2021.07.003](http://doi.org/10.1016/j.ccell.2021.07.003).
11. Zhou J, Xu Y, Lin S, et al. iUUCD 2.0: an update with rich annotations for ubiquitin and ubiquitin-like conjugations. *Nucleic Acids Res* 2018;46(D1):D447-53. [http://doi.org/ 10.1093/nar/gkx1041](http://doi.org/10.1093/nar/gkx1041).
12. Gao T, Liu Z, Wang Y, et al. UUCD: a family-based database of ubiquitin and ubiquitin-like conjugation. *Nucleic Acids Res* 2013;41(Database issue):D445-51. [http://doi.org/ 10.1093/nar/gks1103](http://doi.org/10.1093/nar/gks1103).
13. Brunet JP, Tamayo P, Golub TR, et al. Metagenes and molecular pattern discovery using matrix factorization. *Proc Natl Acad Sci U S A* 2004;101(12):4164-69. [http://doi.org/ 10.1073/pnas.0308531101](http://doi.org/10.1073/pnas.0308531101).

14. Liberzon A, Birger C, Thorvaldsdottir H, et al. The Molecular Signatures Database (MSigDB) hallmark gene set collection. *Cell Syst* 2015;1(6):417-25. [http://doi.org/ 10.1016/j.cels.2015.12.004](http://doi.org/10.1016/j.cels.2015.12.004).
15. Lin W, Wang X, Xu Z, et al. Identification and validation of cellular senescence patterns to predict clinical outcomes and immunotherapeutic responses in lung adenocarcinoma. *Cancer Cell Int* 2021;21(1)[http://doi.org/ 10.1186/s12935-021-02358-0](http://doi.org/10.1186/s12935-021-02358-0).
16. Thorsson V, Gibbs DL, Brown SD, et al. The Immune Landscape of Cancer. *Immunity* 2018;48(4):812-30. [http://doi.org/ 10.1016/j.immuni.2018.03.023](http://doi.org/10.1016/j.immuni.2018.03.023).
17. Li T, Fan J, Wang B, et al. TIMER: A Web Server for Comprehensive Analysis of Tumor-Infiltrating Immune Cells. *Cancer Res* 2017;77(21):e108-10. [http://doi.org/ 10.1158/0008-5472.CAN-17-0307](http://doi.org/10.1158/0008-5472.CAN-17-0307).
18. Li T, Fu J, Zeng Z, et al. TIMER2.0 for analysis of tumor-infiltrating immune cells. *Nucleic Acids Res* 2020;48(W1):W509-14. [http://doi.org/ 10.1093/nar/gkaa407](http://doi.org/10.1093/nar/gkaa407).
19. Wang W, Shao F, Yang X, et al. METTL3 promotes tumour development by decreasing APC expression mediated by APC mRNA N6-methyladenosine-dependent YTHDF binding. *Nat Commun* 2021;12(1)[http://doi.org/ 10.1038/s41467-021-23501-5](http://doi.org/10.1038/s41467-021-23501-5).
20. Baine MK, Hsieh M, Lai WV, et al. SCLC Subtypes Defined by ASCL1, NEUROD1, POU2F3, and YAP1: A Comprehensive Immunohistochemical and Histopathologic Characterization. *J Thorac Oncol* 2020;15(12):1823-35. [http://doi.org/ 10.1016/j.jtho.2020.09.009](http://doi.org/10.1016/j.jtho.2020.09.009).
21. Alomari M. TRIM21 - A potential novel therapeutic target in cancer. *Pharmacol Res* 2021;165:105443. [http://doi.org/ 10.1016/j.phrs.2021.105443](http://doi.org/10.1016/j.phrs.2021.105443).
22. Huang ZD, Lin LL, Liu ZZ, et al. m6A Modification Patterns With Distinct Immunity, Metabolism, and Stemness Characteristics in Soft Tissue Sarcoma. *Front Immunol* 2021;12:765723. [http://doi.org/ 10.3389/fimmu.2021.765723](http://doi.org/10.3389/fimmu.2021.765723).
23. Zhong J, Liu Z, Cai C, et al. m(6)A modification patterns and tumor immune landscape in clear cell renal carcinoma. *J Immunother Cancer* 2021;9(2)[http://doi.org/ 10.1136/jitc-2020-001646](http://doi.org/10.1136/jitc-2020-001646).
24. Li YH, Tong KL, Lu JL, et al. PRMT5-TRIM21 interaction regulates the senescence of osteosarcoma cells by targeting the TXNIP/p21 axis. *Aging (Albany NY)* 2020;12(3):2507-29. [http://doi.org/ 10.18632/aging.102760](http://doi.org/10.18632/aging.102760).
25. Kim H, Frederick DT, Levesque MP, et al. Downregulation of the Ubiquitin Ligase RNF125 Underlies Resistance of Melanoma Cells to BRAF Inhibitors via JAK1 Deregulation. *Cell Rep* 2015;11(9):1458-73. [http://doi.org/ 10.1016/j.celrep.2015.04.049](http://doi.org/10.1016/j.celrep.2015.04.049).
26. Feng J, Zhang Y, Ren X, et al. Leucine-rich repeat containing 4 act as an autophagy inhibitor that restores sensitivity of glioblastoma to temozolomide. *Oncogene* 2020;39(23):4551-66. [http://doi.org/ 10.1038/s41388-020-1312-6](http://doi.org/10.1038/s41388-020-1312-6).
27. Feng J, Ren X, Fu H, et al. LRRC4 mediates the formation of circular RNA CD44 to inhibit GBM cell proliferation. *Mol Ther Nucleic Acids* 2021;26:473-87. [http://doi.org/ 10.1016/j.omtn.2021.08.026](http://doi.org/10.1016/j.omtn.2021.08.026).
28. Fedele M, Sgarra R, Battista S, et al. The Epithelial-Mesenchymal Transition at the Crossroads between Metabolism and Tumor Progression. *Int J Mol Sci* 2022;23(2)[http://doi.org/ 10.3390/ijms23020800](http://doi.org/10.3390/ijms23020800).

29. Sannino G, Marchetto A, Kirchner T, et al. Epithelial-to-Mesenchymal and Mesenchymal-to-Epithelial Transition in Mesenchymal Tumors: A Paradox in Sarcomas? *Cancer Res* 2017;77(17):4556-61. <http://doi.org/10.1158/0008-5472.CAN-17-0032>.

Figures

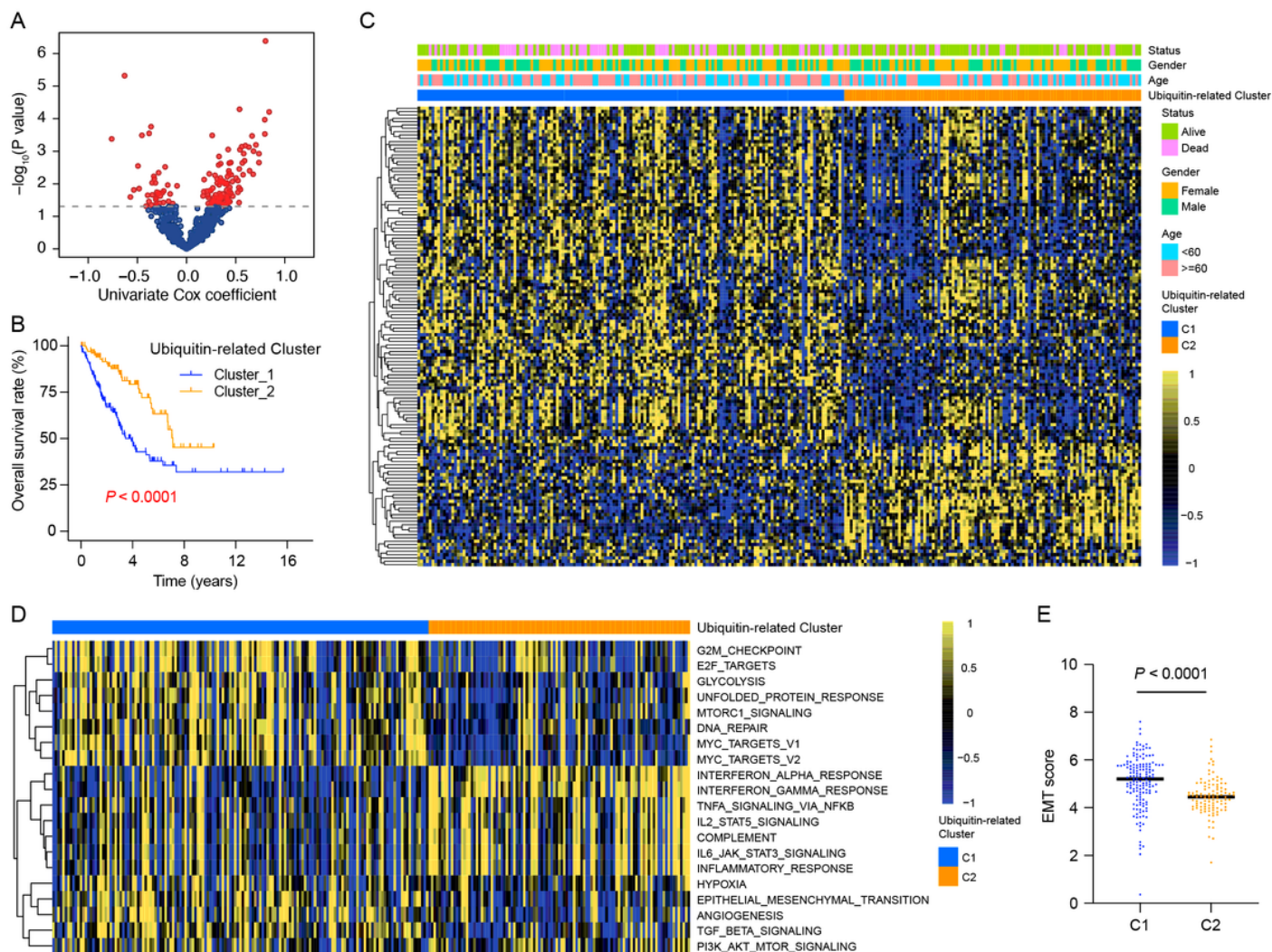


Figure 1

Identification of two ubiquitin-related genes-based clusters with distinct prognoses and biological processes in sarcomas. **A** Volcano plot showing univariate analyses of the ubiquitin-related genes in TCGA-SARC. **B** Kaplan-Meier survival analyses of patients in different clusters. **C** Heatmap showing the expressions of ubiquitin-related genes in patients with different survival status, gender, and age from TCGA-SARC. **D** Gene set variation analysis of hallmark pathways in different clusters. **E** Comparison of EMT scores in different clusters. TCGA-SARC, The Cancer Genome Atlas sarcoma cohort; EMT, epithelial-mesenchymal transition.

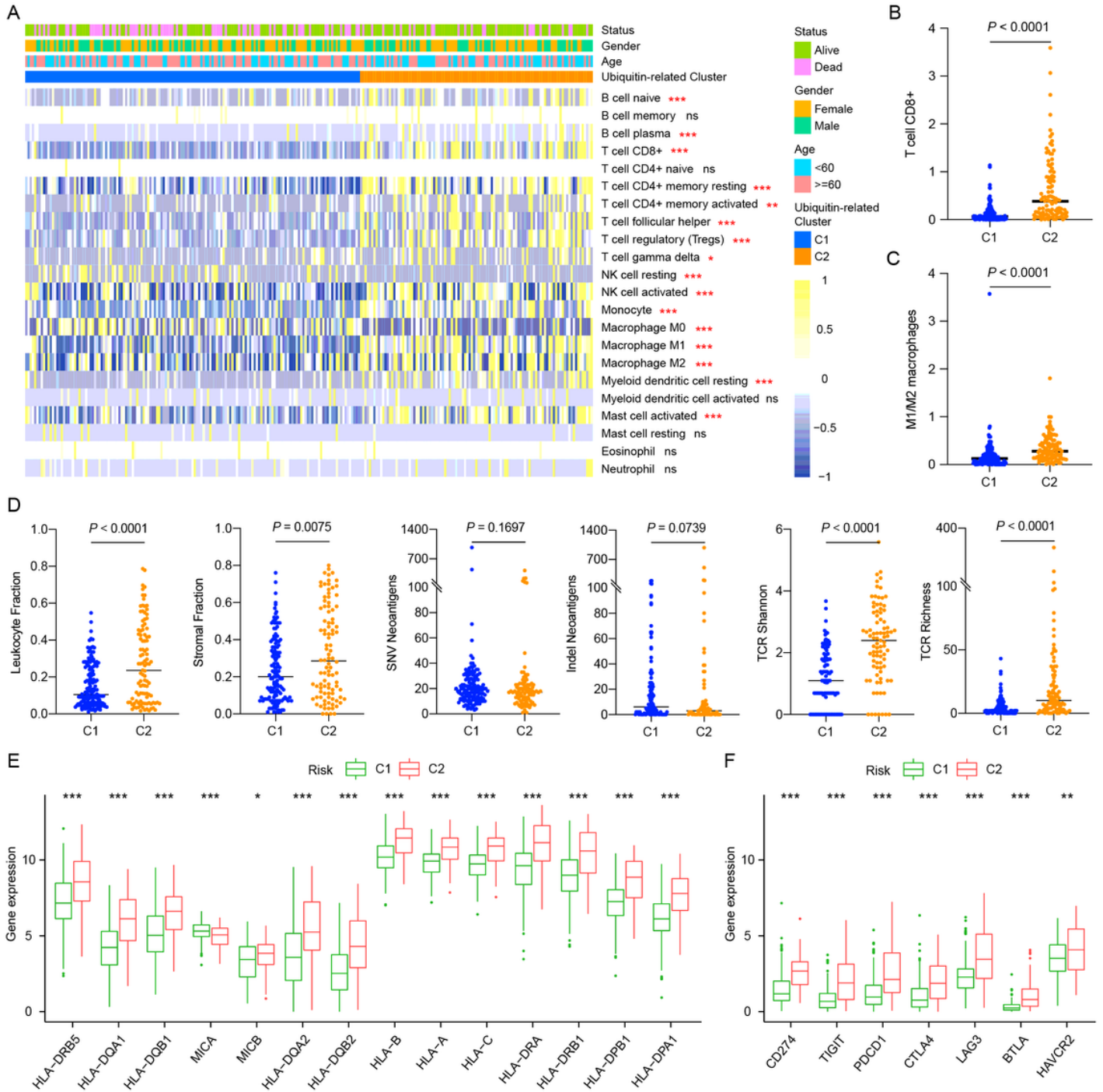


Figure 2

Comparison of the tumor environment between two ubiquitin-related genes-based clusters. **A** Heatmap showing the abundance of different immune cell types in the two clusters. **B-C** Comparison of CD8+ T cell infiltration levels and M1/M2 macrophage proportions between the two clusters. **D** Comparison of leukocyte fraction, stromal fraction, SNV neoantigens, indel neoantigens, TCR stromal, and TCR richness

between the two clusters. **E-F** Comparison of antigen presentation-related gene expressions and prominent checkpoints gene expressions between the two clusters.

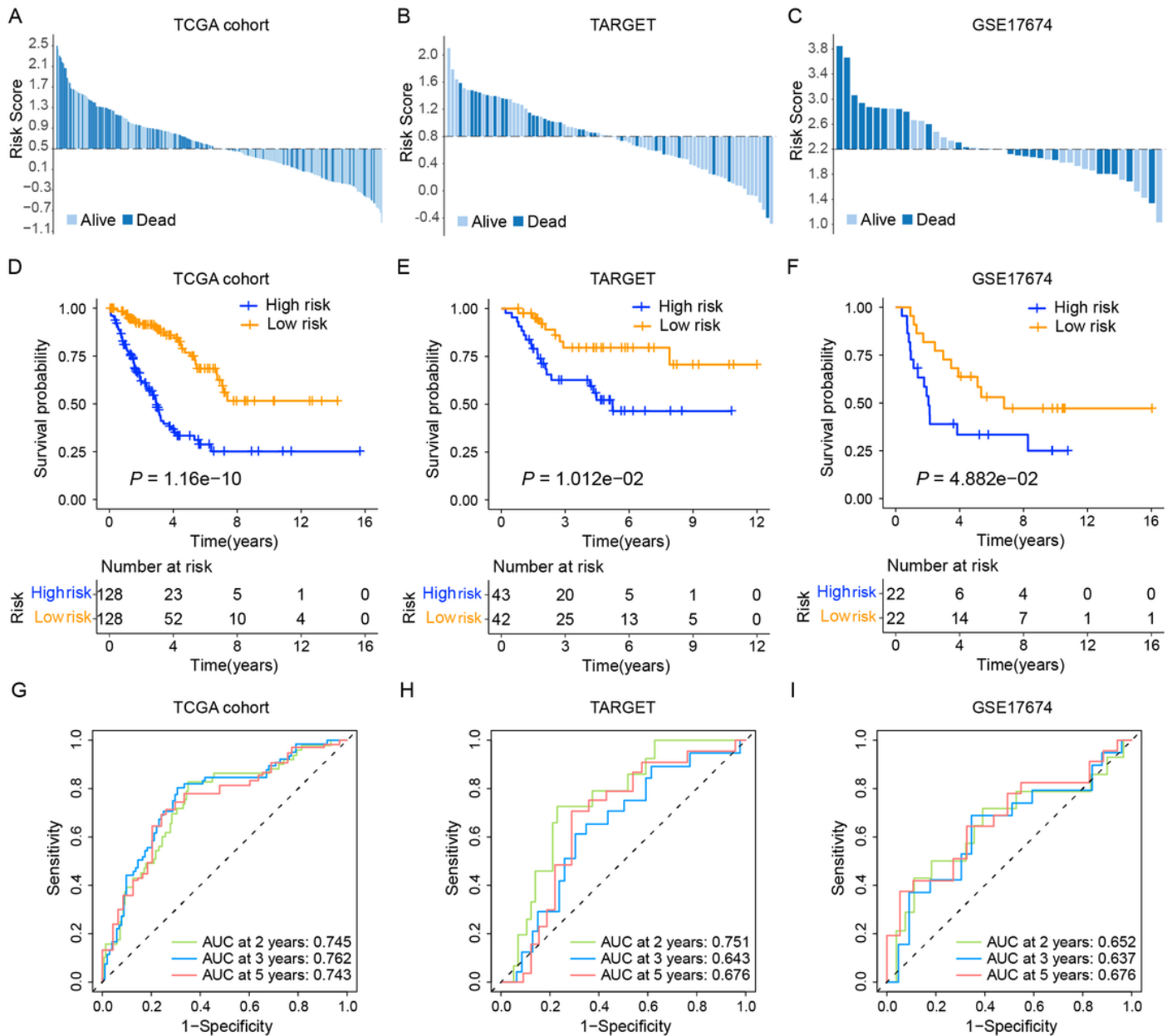


Figure 3

Construction and validation of a ubiquitin-related signature in three public datasets. **A-C** Distribution of the risk scores of patients in the datasets. **D-F** Kaplan-Meier survival analyses of patients from different risk groups in the datasets. **G-I** Receiver operating characteristic curves assessing the performance of the signature in the datasets.

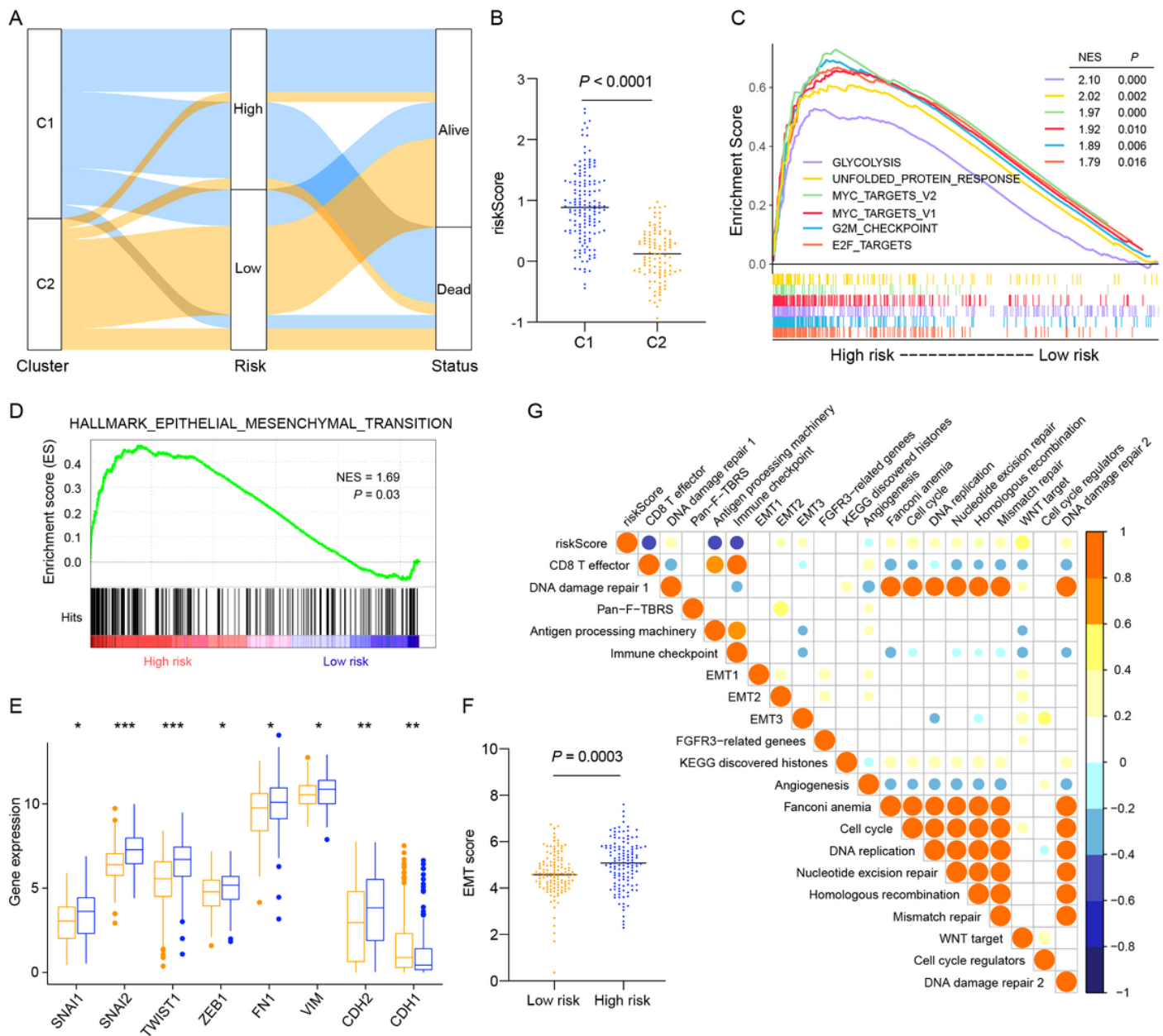


Figure 4

Characterization of patients from different risk groups in TCGA-SARC. **A** Alluvial diagram depicting relations of ubiquitin clusters, different risk groups, and survival status. **B** Comparison of risk scores between the two clusters. **C** Gene set enrichment analyses of hallmark pathways in different risk groups. **D** Gene set enrichment analyses of the hallmark of EMT pathway in different risk groups. **E-F** Comparisons of the expressions of EMT-related genes and EMT scores between the two risk groups. **G** Correlations between the signature and the known gene signatures in TCGA-SARC patients. TCGA-SARC, The Cancer Genome Atlas sarcoma cohort; EMT, epithelial–mesenchymal transition.

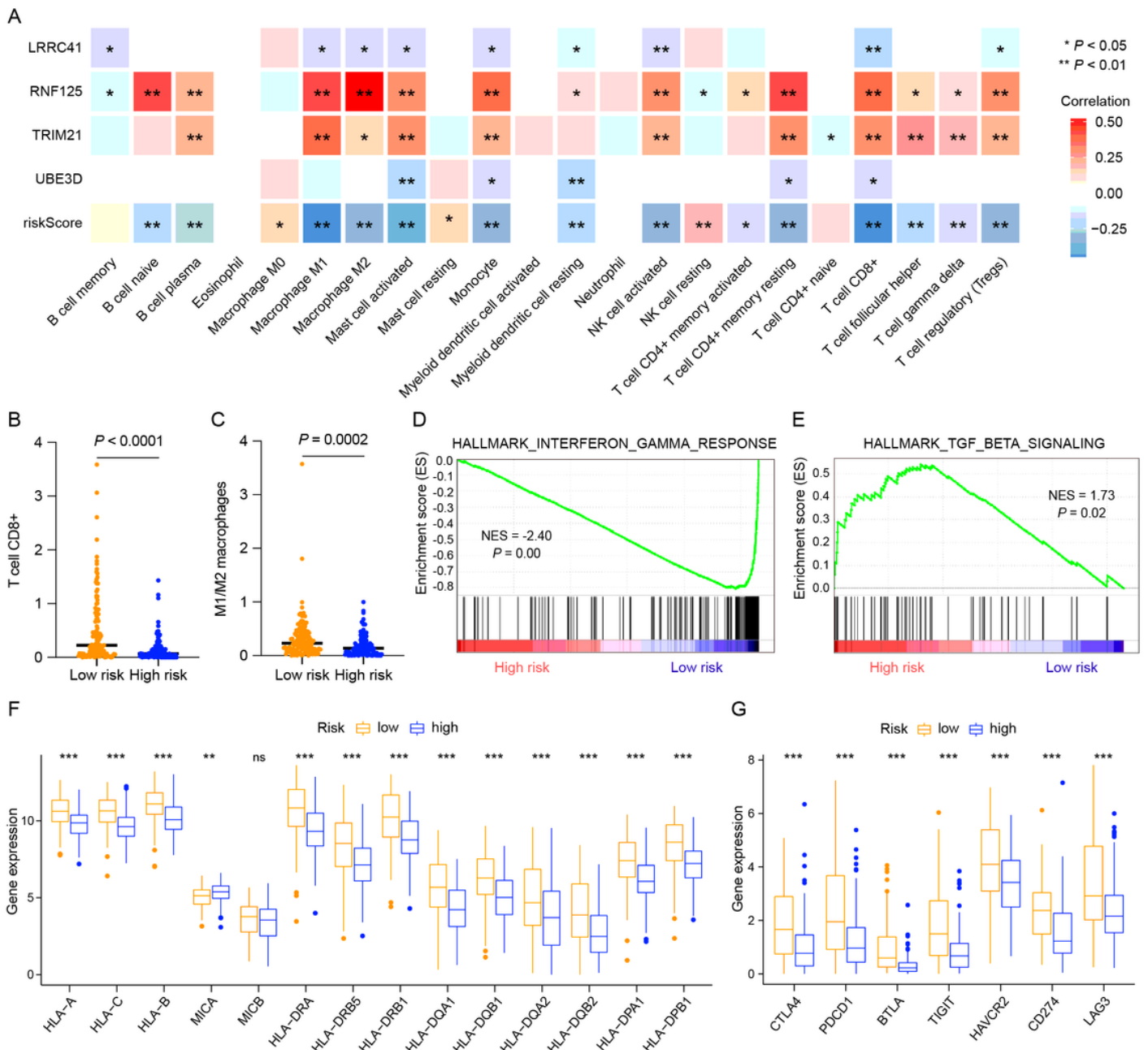


Figure 5

Characterization of the tumor environment between different risk groups. **A** Correlations between the infiltrating immune cells and four signature genes, risk score. **B-C** Comparisons of CD8+ T cell infiltration levels and M1/M2 macrophage proportions between different risk groups. **D-E** Gene set enrichment analyses of the hallmarks of interferon-gamma response and TGF-beta signaling in different risk groups. **F-G** Comparison of antigen presentation-related gene expressions and prominent checkpoints gene expressions between different risk groups.

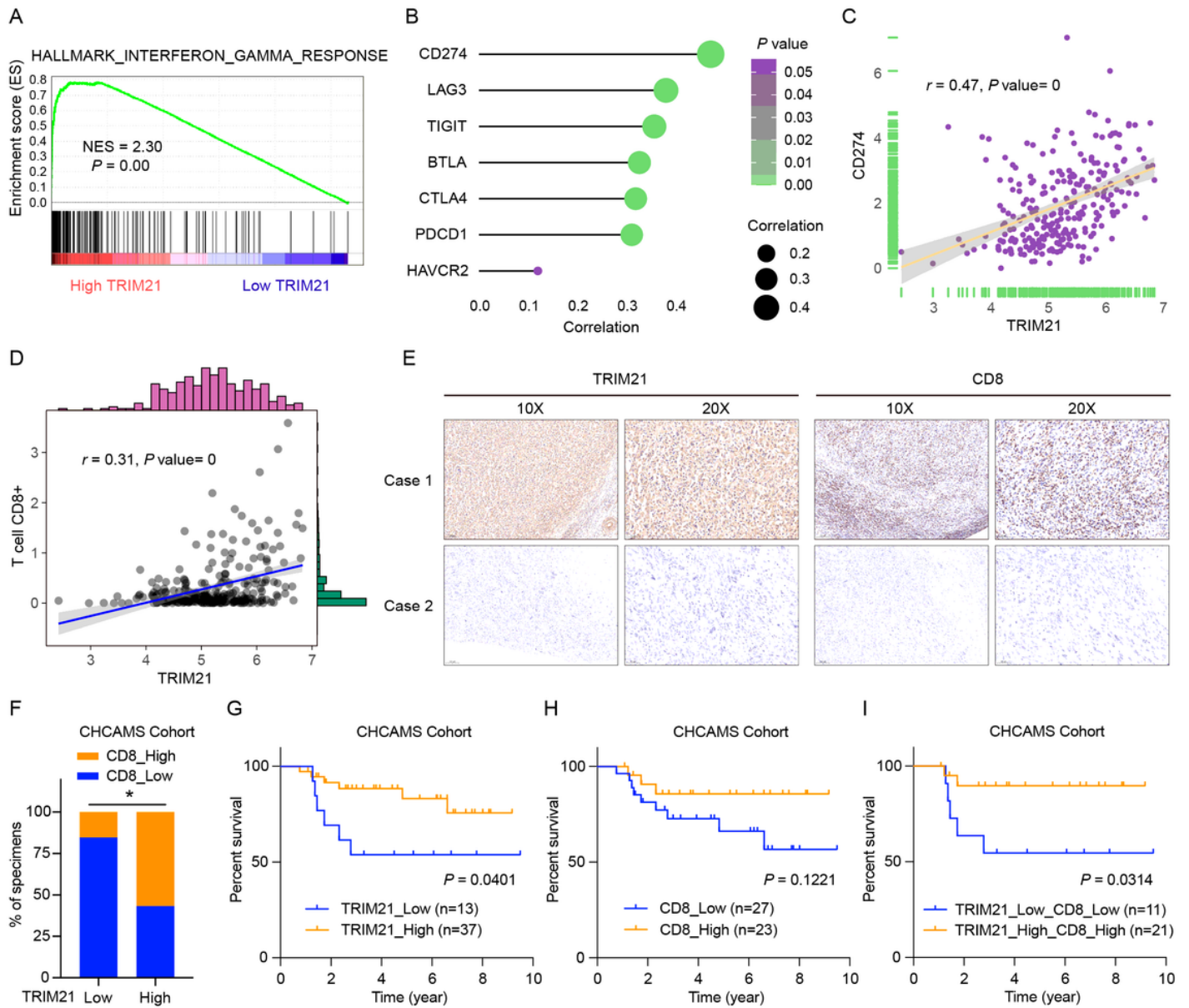


Figure 6

Analyses for TRIM21 and validation in an independent cohort. **A** Gene set enrichment analyses of the hallmark of interferon-gamma response in TCGA-SARC patients with different TRIM21 expressions. **B** Correlations between TRIM21 and prominent checkpoint genes in TCGA-SARC patients. **C-D** The correlations between TRIM21 and CD274, CD8+ T cells in TCGA-SARC patients. **E** Representative immunohistochemistry images of TRIM21 and CD8 from an alive case (case 1) and a deceased case (case 2) in our independent cohort. **F** The correlation between TRIM21 and CD8 in our cohort. **G-I** Kaplan-Meier survival analyses of patients stratified by TRIM21, CD8, and both TRIM21, CD8 expressions in our cohort. TCGA-SARC, The Cancer Genome Atlas sarcoma cohort; CHCAMS, Cancer Hospital, Chinese Academy of Medical Sciences.

Supplementary Files

This is a list of supplementary files associated with this preprint. Click to download.

- [supplementaryfile.zip](#)